Water in Glassy Carbohydrates: Opening It Up at the Nanolevel

Duncan Kilburn,[†] Johanna Claude,[‡] Raffaele Mezzenga,[‡] Gunter Dlubek,[†] Ashraf Alam,[†] and Job Ubbink*[,‡]

H. H. Wills Physics Laboratory, University of Bristol, Tyndall Avenue, Bristol BS8 1TL, United Kingdom, and Nestlé Research Center, Vers-chez-les-Blanc, CH-1000 Lausanne 26, Switzerland

Received: March 18, 2004; In Final Form: June 14, 2004

Sorption of water by glassy biopolymers and the effects of absorbed water on molecular mobility including plasticization, matrix rearrangements, and diffusion are poorly understood mainly because molecular and structural analyses are scarce. Here, we report the first investigation of the nanostructure of amorphous carbohydrates and the plasticizing effects of water by combining positron annihilation lifetime spectroscopy (PALS) and thermodynamic analysis. Surprisingly, we find that the average volume of the voids between the polymer chains increases with the water content of the matrix while the density of the matrix increases. Consequently, the free volume of the carbohydrate matrix decreases continuously up to the glass transition, primarily by the filling or elimination of the smallest intermolecular voids. We conclude that a so far unknown length scale, the typical size of intermolecular voids, is of fundamental importance in understanding the interaction of water with amorphous carbohydrates and their ensuing plasticization.

Introduction

Plasticization of amorphous carbohydrates by water is an ubiquitous phenomenon influencing the stability and functionality of pharmaceutical excipients, food products, and controlled release systems.[1−5] Water is a highly efficient plasticizer of carbohydrates and the glass transition temperature of an amorphous carbohydrate matrix decreases strongly as a function of the water content.[6] The diffusional mobility of small molecules such as water,[7−9] gases,[10] or volatile organic compounds[11] increases rapidly with increasing water content in both the glassy and rubbery states. Yet, little is known about the molecular mechanism of water sorption and plasticization of amorphous carbohydrates.

We present the first nanostructural investigation of an amorphous carbohydrate glass, and the influence of water on the physical structure at the nanoscale. To acquire a fundamental picture of water−polysaccharide interactions in dense matrixes, thermodynamic analysis is combined with Positron Annihilation Lifetime Spectroscopy (PALS). PALS is a powerful technique used to study the size distribution of voids in dense materials on subnanometer length scales[12−14] and is the only well-established technique by which the structure of dense disordered materials can directly be probed.

Thermodynamic Relations

The system under consideration consists of two constituents: the (polydisperse) glucose polymer and water. At a given temperature T, the state of the matrix may macroscopically be characterized by its density and its composition. The density, ρ, is defined by

$$\rho = M/V \tag{1}$$

with M the mass of the system and V its volume.

From an experimental point of view, a convenient way to express the composition of the system is in terms of the weight fractions of polymer and water:

$$Q_{\mathrm{pol}} = \frac{m_{\mathrm{pol}}}{m_{\mathrm{pol}} + m_{\mathrm{w}}}; \qquad Q_{\mathrm{w}} = \frac{m_{\mathrm{w}}}{m_{\mathrm{pol}} + m_{\mathrm{w}}} \tag{2}$$

where m_{pol} is the weight of polymer and m_{w} the weight of water in the system and $Q_{\mathrm{pol}} + Q_{\mathrm{w}} = 1$.

As sorption isotherms are generally expressed in terms of the amount of water adsorbed per unit weight of polymer matrix, we will need the expression for the weight ratio of water to polymer:

$$Q' = m_{\mathrm{w}}/m_{\mathrm{pol}} \tag{3}$$

The mole numbers of monomer and water are defined by

$$n_{\mathrm{pol}} = m_{\mathrm{pol}}/M_{\mathrm{pol}}; \qquad n_{\mathrm{w}} = m_{\mathrm{w}}/M_{\mathrm{w}} \tag{4}$$

where M_{pol} and M_{w} are the molecular weights of monomer and water, respectively. In case of maltodextrin, the effective monomer is anhydroglucose with a molecular weight $M_{\mathrm{pol}} = 162$ Da.

The degree of volumetric swelling is defined by

$$\theta = \frac{V}{V_0} = \frac{\rho_0}{\rho}\frac{1}{Q_{\mathrm{pol}}} \tag{5}$$

The reference state is the dry system, referred to by the subscript "0".

The partial molar volumes of polymer and water are defined by[15]

$$\bar{v}_{\mathrm{pol}} = \left(\frac{\partial V}{\partial n_{\mathrm{pol}}}\right)_{T,p,n_{\mathrm{w}}}; \qquad \bar{v}_{\mathrm{w}} = \left(\frac{\partial V}{\partial n_{\mathrm{w}}}\right)_{T,p,n_{\mathrm{pol}}} \tag{6}$$

where T is the absolute temperature and p is the pressure.

* Corresponding author. E-mail: johan.ubbink@rdls.nestle.com.
[†] University of Bristol.
[‡] Nestlé Research Center.

10.1021/jp048774f CCC: $27.50
Published on Web 07/22/2004

For water, the partial molar volume may be expressed as

$$\bar{v}_w = \left(\frac{\partial V}{\partial n_w}\right)_{T,p,n_p} = \frac{M_w}{\rho_0}(1 - Q_w)^2 \frac{\partial \theta}{\partial Q_w} = \frac{M_w}{\rho_0}\frac{\partial \theta}{\partial Q'} \quad (7)$$

The volume fraction of water in the polymer matrix is then given by[15]

$$\phi_w = \frac{V_w}{V} = \frac{\bar{v}_w Q_w \rho}{M_w} \quad (8)$$

with $\phi_p + \phi_w = 1$.

The sorption of water by the polymer matrix can be quantified by using a large number of isotherm models of which the Guggenheim−Anderson−de Boer (GAB) isotherm has turned out to be the most versatile:[6]

$$Q' = \frac{KCW_m a_w}{(1 - Ka_w)(1 - Ka_w + KCa_w)} \quad (9)$$

where K, C, and W_m are constants characterizing the system.

The GAB isotherm, which is an extension of the BET isotherm,[17] is well suited to fit the sigmoidal water sorption isotherms observed for biopolymer matrixes in both the glassy and rubbery states.

In addition, to model the sorption of water in the glassy state of the polymer matrix, we will make use of the Freundlich isotherm[19]

$$Q' = Ka_w^{1/c} \quad (10)$$

where the system is characterized by the constants K and c ($c \geq 1$).

The Freundlich model is generally found to be applicable for the sorption on rigid, heterogeneous absorbates.[19] This is what we would anticipate for glassy systems.

From the adsorption isotherm and the density of the system, the Zimm−Lundberg clustering function of the solvent in the polymer matrix may be calculated:[18]

$$\frac{G_{ww}}{\bar{v}_w} = -\phi_p\left[\frac{\partial(a_w/\phi_w)}{\partial a_w}\right]_{T,p} - 1 \quad (11)$$

where the coefficient $G_{ww}/\bar{v}_w$ signifies the degree of clustering of the solvent molecules in the polymer matrix. The subscript "w" denotes the solvent, which is water in our case. Positive values of the clustering function indicate that the water in the matrix forms small clusters or pockets between the polymer chains. Conversely, strongly negative values of the clustering function signify a highly disperse state of water in the matrix. For $G_{ww}/\bar{v}_w = -1$, the distribution of water in the matrix is as for a random distribution of noninteracting solvent molecules.

Materials and Methods

Preparation of Matrices. Maltodextrin DE-12, a mixture of α-(1→4) linked glucose oligosaccharides with occasional α-(1→6) branches derived from starch by acid hydrolysis (Glucidex IT-12, weight-average molecular weight $M_w = 18.6 \times 10^3$ Da; lot no. E8950, Roquette Freres, Lestrem, France), was dissolved in demineralized water at 60 °C at a total solids content of 70 wt % using a Stephan VM60 mixer (Stephan, Germany). After dissolution by slow stirring (approximately 1 rpm) for 1−2 h, the sample was slowly concentrated by evaporation under reduced pressure (approximately 200 mbar) until the viscosity of the solution became too high for the mixer (about 6 h). The concentrated solution was then transferred into stainless steel trays (layer thickness approximately 1 cm) and dried at 60 °C under reduced pressure (400 mbar) in a Vacutherm vacuum oven (Hereaus Instruments, Germany). The sample was dried until it was in or close to the glassy state at room temperature, ground with a Frewitt mill (Urschell, Germany) (mesh sizes 500 and 800 μm), and further dried at 60 °C and 400 mbar of pressure until a final water activity of about 0.1 was reached. The ground sample was sieved into size fractions by using a series of analytical sieves (Retsch, Germany) and the size fraction between 200 and 300 μm was used for water-activity equilibration and all further experiments.

Sample Equilibration. Samples were equilibrated at various water activities in desiccators containing saturated salt solutions of known relative humidity ($a_w = 0.11$ ($LiCl$), 0.22 (CH_3COOK), 0.33 ($MgCl_2$), 0.43 (K_2CO_3), 0.54 ($Mg(NO_3)_2$), and 0.75 ($NaCl$)) (Greenspan, 1977). The equilibration was carried out at 25 ± 1 °C and the sorption of water was determined gravimetrically. The equilibration was achieved within a storage time of 35 days. Samples for PALS experiments were prepared by compaction of about 0.1 g of equilibrated powder into a disk (diameter 1 cm, thickness ∼1.1 mm) with a laboratory press.

Determination of Water Content. The water content was determined gravimetrically using a home-built apparatus comprising glass vacuum tubes containing the desiccant P_2O_5 which are immersed in an oil bath. Water was fully extracted from the samples after drying for 6 h at 102 °C in the presence of P_2O_5 (Merck, Germany) at a reduced pressure of 25 mbar as confirmed by the absence of a water peak at $\lambda = 1940$ nm in near infrared reflectance spectroscopy (Infra-analyzer 500, Bran + Lübbe, Germany). The variation between duplicates was <0.1% w/w on initial weight.

Measurement of Water Activity. The initial water activity of the samples was measured in duplicate with a humidity sensor (Hygroscop DT, Rotronic AG, Switzerland) kept at 25.0 ± 0.1 °C and calibrated with saturated salt solutions of known relative humidity (see above). The signal was recorded for at least 1 h to ensure that thermodynamic equilibrium was established. The variation between the duplicates was <0.005.

Analysis of Glass Transition by Differential Scanning Calorimetry (DSC). Calorimetric measurements were carried out on a Seiko 220C DSC (Seiko, Japan) with a heating rate of 5 deg/min and a cooling rate of 25 deg/min. A stabilization time of 1 min was applied for every 10 °C the sample was cooled after the first heating run. The analyses were carried out with approximately 20 mg of sample hermetically sealed in an aluminum pan (P/N SSC000E031, Seiko, Japan). An empty aluminum pan was used as a reference. The T_g was determined from the onset of the change in heat flow observed at the second heating ramp.

Determination of Density. The density ρ_a of the samples was determined with an Accupyc 1330 pycnometer (100-mL cell with 10-mL insert) (Micromeritics, USA). Helium was used as displacement gas at an equilibration rate of 0.1 kPa/min. For values of the density significant up to the third decimal place, 10 sample runs were found sufficient.

PALS Experiments and Analysis. A new sample holder was designed to facilitate the measurement of positron lifetimes with no loss of water from the sample. The sample holder was made of high conductivity copper and allowed full temperature control via a resistive heater. The cavity in which the sample is located has dimensions 30 mm (height) × 12 mm (width) × 4 mm

(depth), which was judged to be sufficiently large to provide accurate water content control.

Positron annihilation lifetime measurements were carried out on a fast-fast lifetime spectroscope with a Gaussian resolution function having a FWHM of 280 ps. The source of the positrons was sodium-22 prepared by depositing ^{22}NaCl onto 8 μm thick Kapton foil. A compressed disk is placed on either side of the source and the sample cavity was subsequently filled with powder equilibrated at the same water activity as the sample disks to minimize moisture transfer within the sample cell. The thickness of the sample disks, about ~1.1 mm, is enough to stop ~99% of the positrons. Data were collected over a period of 2 h giving ~1×10^6 counts per spectrum. The source components we measured were 7.99% of the total spectrum at 363 ps and 0.54% at 3400 ps; these were removed from all measured spectra prior to analysis. Assuming that the holes are, on average, spherical in shape, the pick-off lifetime can be related by a simple semiempirical quantum mechanical model to the radius of the hole, quantified in the so-called Tao-Eldrup formula[13,33]

$$\tau_{o-\mathrm{Ps}} = \frac{\tau_{\mathrm{av}}}{1 - \frac{r}{r+\delta r} + \frac{1}{2\pi}\sin\left(\frac{2\pi}{r+\delta r}\right)} \qquad (12)$$

where τ_{av} is the spin-averaged positronium annihilation lifetime ($\tau_{\mathrm{av}} = 0.5$ ns) and r is the radius of the hole. A value of $\delta r = 0.166$ nm is widely accepted and was determined empirically by fitting eq 12 to the ortho-Positronium (o-Ps) lifetime observed for free volume holes of known size in various porous materials.[13] The total spectrum is a sum of lifetime components, τ_i, weighted by the relevant intensity, I_i, convoluted with a resolution function, $R(t)$, plus a background, B. This is described by

$$S(t) = \left[R(t)\sum\left(\frac{I_i}{\tau_i}\right)\exp\left(-\frac{t}{\tau_i}\right)\right] + B \qquad (13)$$

The three lifetimes, para-Ps self-annihilation, free positron annihilation, and o-Ps "pick-off" annihilation, are labeled τ_1, τ_2, and τ_3, respectively. Fitting to the above equation, with discrete components, will yield the mean of the void distribution.

Results and Discussion

In Figure 1, the volume of the voids or holes as determined from the PALS experiments is shown for dense matrices of maltodextrin as a function of the temperature. The maltodextrin, which is a polymer of glucose derived from starch, is probed at various water contents; at equilibrium at 25 °C, each specific water content corresponds to the water activity a_w indicated in Table 1. The average hole volume V_h increases linearly with temperature up to a critical temperature where the slope suddenly increases. The increase of the hole volume as a function of temperature is significant: for the sample with $a_w = 0.75$ at 25 °C, the average hole volume is about 30 Å^3 at −100 °C, increasing to 69 Å^3 at the crossover temperature and increasing further to about 95 Å^3 at 70 °C. Similar behavior is observed for the samples equilibrated at the other water activities.

We identified that this crossover between the linear low- and high-temperature expansion of the matrix voids occurs at the glass transition temperature T_g of the matrix, as is confirmed by comparison with the T_g determined by differential scanning calorimetry (Figure 2). The glass transition temperature is determined from the PALS data as the intersection of the linear regression of the low-temperature branch and the high-temperature branch (Table 2). The correlation of the linear fit to the experimental data is very good both below and above the glass transition temperature (Table 2).

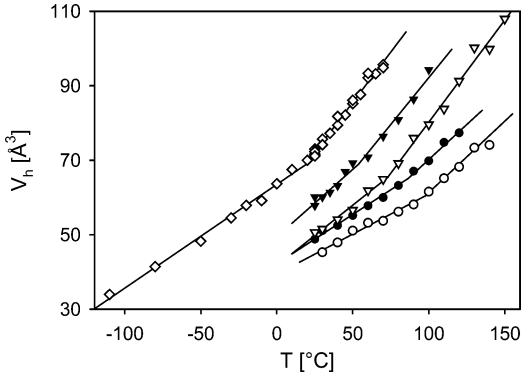

Figure 1. Mean hole volume as a function of the temperature at various water concentrations: open circles: $Q_w = 0.0584$ ($a_w = 0.11$ at 25 °C); filled circles, $Q_w = 0.0730$ ($a_w = 0.22$ at 25 °C); open triangles, $Q_w = 0.0838$ ($a_w = 0.33$ at 25 °C); filled triangles, $Q_w = 0.0924$ ($a_w = 0.54$ at 25 °C); open diamonds, $Q_w = 0.1291$ ($a_w = 0.75$ at 25 °C). The coefficients of the linear regression of the experimental data are given in Table 2 for $T < T_g$ and $T > T_g$.

TABLE 1: Thermodynamic Characterization of the Glassy State of Maltodextrin DE-12 at $T = 25$ °C

a_w	ρ [g·cm^{-3}]	Q_w	ϕ_w	T_g [°C][a]	θ
0	1.5091	0	0	200	1
0.11	1.5255	0.0584	0.0434	97.7	1.051
0.22	1.5351	0.0730	0.0545	86.9	1.060
0.33	1.5406	0.0838	0.0628	73.7	1.069
0.43	1.5438	0.0924	0.0694	64.5	1.077
0.54	1.5508	0.0992	0.0747	50.6	1.080
0.75	1.5612	0.1291	0.0980	17.1	1.110

[a] T_g(onset) from DSC as determined from the 2nd heating run (at 5 deg/min).

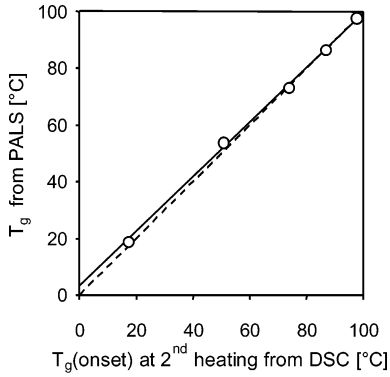

Figure 2. Comparison of the glass transition temperatures from PALS and DSC for various water concentrations: dashed line, slope = 1; solid line, linear regression; $R^2 = 0.999$.

The mean hole volume is found to increase linearly with increasing water content (Figure 3). This is surprising as it is accompanied by an increase in density of the carbohydrate glass (Figure 4). This density increase of carbohydrates upon the sorption of water in the glassy state is presumably a general phenomenon as it was recently also observed for other carbohydrates[20−22] and it is accompanied by a decrease in the free volume of the carbohydrate glass.[20] The monotonic increase in density over the whole range of water content up to 13% suggests that water is strongly bound to the polysaccharide, most likely via the formation of hydrogen bonds with the free hydroxyl groups on the sugars.

TABLE 2: Linear Regression of PALS Data below and above the Glass Transition Temperature[a]

a_w at 25 °C	slope $T < T_g$ [Å³·K⁻¹][b]	R^2	T_g [°C][c]	slope $T > T_g$ [Å³·K⁻¹][b]	R^2
0.11	0.215	0.98	97.6	0.384	0.97
0.22	0.265	0.99	86.4	0.376	0.97
0.33	0.325	0.98	73.0	0.548	0.98
0.54	0.362	0.89	53.7	0.503	0.97
0.75	0.278	0.99	18.9	0.539	0.99

[a] The glass transition temperature is determined self-consistently from a linear regression of the data in the glassy and rubbery states. [b] Slope of the linear regression of the hole volume versus temperature. [c] Defined as the temperature of intersection of the linear regression of the data in the rubbery and glassy states.

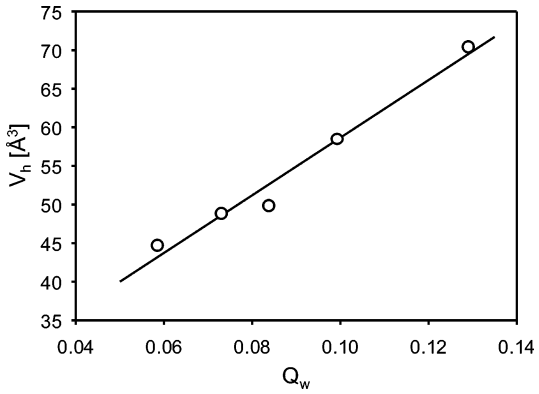

Figure 3. Mean hole volume from the PALS experiments as a function of the water content. Correlation coefficient of the linear fit $R^2 = 0.97$. $T = 25$ °C.

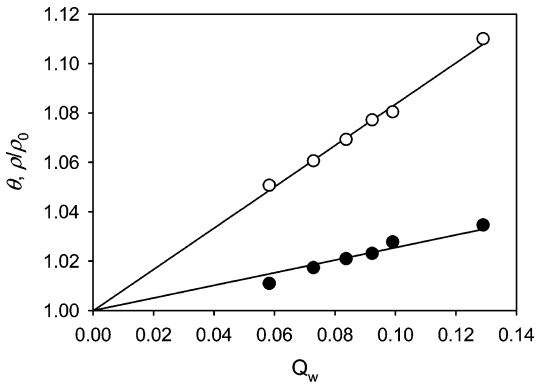

Figure 4. Degree of matrix swelling θ and density increase ρ/ρ_0 as a function of the weight fraction of water Q_w: open symbols, θ; filled symbols, ρ/ρ_0. The lines represent the linear regression of the data: $R^2 = 0.998$ (θ vs Q_w); $R^2 = 0.982$ (ρ/ρ_0 vs Q_w). $T = 25$ °C.

The water sorption isotherm of the dense granules of maltodextrin DE-12 in the glassy state can be well fitted by using the Freundlich model, whereas a satisfactory fit of the water sorption in both the glassy and rubbery states is obtained with use of the GAB model (Figure 5a). The fitting parameters for the two isotherm models are given in Table 3. The data point at $a_w = 0.54$ deviates considerably from the optimal GAB fit, whereas it fits very well with the Freundlich model. Within a linear interpolation of the glass transition data in the range of $0.11 \leq a_w \leq 0.75$, the water activity at which the T_g is 25 °C is 0.72. Consequently, all data points in the range $0 \leq a_w \leq 0.54$ are in the glassy state for which the water sorption behavior should be according to the Freundlich model, as is indeed observed. Deviations from the Freundlich model become pronounced as soon as the critical water activity for which the glass transition is equal to the equilibration temperature is crossed (Figure 5a).

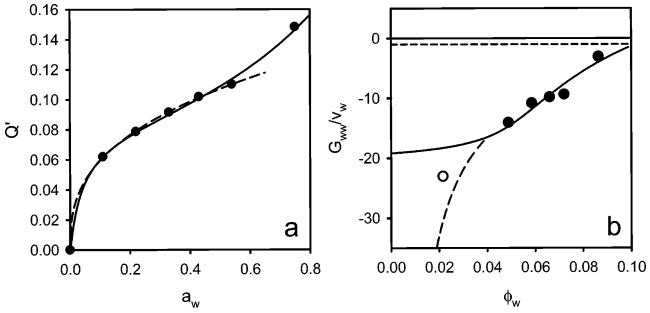

Figure 5. (a) Water sorption isotherm of the maltodextrin matrix at 25 °C. (b) Zimm−Lundberg clustering function[18] of water as function of the volume fraction of water. The solid lines are drawn using the GAB model for sigmoidal sorption isotherms[6] and the dashed lines using the Freundlich model for rigid site adsorption.[19] The Freundlich isotherm is solely used to model the glassy state ($0 \leq a_w \leq 0.54$). In part b, only the low-water content part of the clustering function according to the Freundlich model is shown. The open symbol denotes the data point calculated assuming $a_w/\phi_w = 0$ at $a_w = 0$. The state $G_{ww}/v_w = -1$, where the distribution of water is as if random, is indicated by a dotted line. It is clear that in the glassy state, water is closely associated with the carbohydrate polymer and not with itself ($G_{ww}/v_w \ll -1$).

TABLE 3: Fitting Coefficients of the Water Sorption Isotherm of Dense Granules of Maltodextrin DE-12 for the GAB and Freundlich Models

GAB model		Freundlich model		
a_w range	residue[a]	a_w range	residue[a]	
0−0.75	1.86×10^{-5}	0−0.54	1.02×10^{-6}	
GAB model			Freundlich model	
K	C	W_m	K	c
0.6571	40.60	0.07762	0.1379	2.735

[a] $\sum_n (Q'_{exp,n} - Q'_{mod\ el,n})^2$.

TABLE 4: Zimm−Lundberg Clustering Function for Maltodextrin DE-12 in the Glassy State ($T = 25$ °C)

ϕ_w	$G_{ww}/\bar{v}_w$
0.0217	−23.1
0.0489	−14.1
0.0587	−10.8
0.0662	−9.85
0.0721	−9.41
0.0865	−3.09

From the water sorption isotherm (Figure 5a) and the relation between the density and the water content (Figure 4), we calculate the partial molar volume to be 8.7 cm³/mol for all samples in the glassy state. This low value of the partial molar volume of water should be compared to its value in the liquid state (18 cm³/mol) and the molar volume derived from the estimated van der Waals volume of the water molecule (11.7 Å³, corresponding to a molar volume of 7.1 cm³/mol [23]). In the glassy carbohydrate matrix, water consequently exists in a strongly nonideal state, as is confirmed by a Zimm−Lundberg clustering analysis of the water sorption isotherm (Figure 5b; Table 4).

The density of the carbohydrate matrix, which increases from 1.51 g/cm³ at $a_w = 0$ to 1.55 g/cm³ at $a_w = 0.54$ in the glassy state, initially continues to rise in the same linear fashion in the rubbery state (viz. the value of 1.56 g/cm³ at $a_w = 0.75$; Figure 4). Consequently, the partial molar volume of water in the initial part of the rubbery state is about ∼9 cm³/mol, i.e., close to its value in the glassy state. Naturally, at very high water contents, the density will start to decrease to finally reach the value of liquid water in the concentration limit of zero

carbohydrate and the partial molar volume of water will rise concomitantly.[20]

From the experimental point at $\phi_w \approx 0.02$ (open symbol in Figure 5b), one could be inclined to believe that the asymptotic behavior of the clustering function to low water content is more appropriately represented using the Freundlich model. However, the precise value of this data point is dependent on the assumed initial value for a_w/ϕ_w at low water content. Limiting values for a_w/ϕ_w at low water content vary substantially, depending on the asymptotic behavior of the isotherm model. Whereas for the Freundlich model, $\phi_w \sim a_w^{1/c}$ for $a_w \rightarrow 0$, where c is of order 1, the asymptotic behavior of the GAB model is $\phi_w \sim KCW_m a_w - K^2C^2W_m a_w^2$ for $a_w \rightarrow 0$, $W_m \ll 1$, $K \leq 1$, and $C \gg 1$. The clustering function $G_{ww}/\bar{v}_w$ therefore tends toward a constant value for the GAB model for $\phi_w \rightarrow 0$. For the Freundlich model, on the other hand, $G_{ww}/\bar{v}_w$ diverges as $\sim a_w^{-1/c}$ for $\phi_w \rightarrow 0$.

As the experimental point at $\phi_w \approx 0.02$ (open symbol in Figure 5b) is calculated assuming $a_w/\phi_w = 0$ it will naturally deviate from the predictions of the GAB model. However, if the clustering function diverges to strongly negative values at low volume fractions of water is not clear from the present state of knowledge, as sufficiently precise water content and water activity determinations in the close-to-dry state have not yet been performed. This is primarily the case because equilibration times, both during sample preparation and during the experimental determination of the water activity with use of headspace sensors, will become prohibitively long as the diffusion coefficient of water in amorphous carbohydrates decreases exponentially with decreasing water content.[6,7] It should be noted that a generalized form of the Freundlich isotherm has been used before in the analysis of the clustering function in amorphous carbohydrates.[24] However, here again the lowest volume fraction of water is too high to substantiate the divergence of the clustering function toward low water content on the basis of the Freundlich model.

The uptake of water leads to a substantial expansion of the volume of the matrix, even in the glassy state, as is shown in Figure 4. The volumetric expansion is a linear function of the water content; from the fully dry state to a system containing 13% water, the matrix expands by 11%. At this latter water content, the system is already in the rubbery state.

The sorption of water by the carbohydrate glass in principle depends on the conditions at which the matrix was brought into the glassy state as the specific molecular packing in one particular realization of the glassy state may influence the number of binding sites for water. The true equilibrium state of a glassy material cannot be reached within in reasonable time frame because of kinetic constraints. However, realizations of the glassy state close to the hypothetical reference state are conventionally generated either by solvent casting and slow evaporation[25] (as in the present paper) or by thermally quenching from the rubbery state.[22,25] For our proposed mechanism of plasticization to remain valid, we should ascertain that our matrices are sufficiently close to the reference state. At the highest water activity investigated, the carbohydrate matrix is in the rubbery state. Consequently, all structural and physical properties have attained their equilibrium values, because of the rapid molecular relaxation and the long equilibration times (>1 month). As for our matrices, the physical properties either change in a continuous way below and above the glass transition (e.g. the density) or remain constant (e.g. the partial molar volume); we conclude that our matrices are close to the reference state even below the glass transition temperature.

From the PALS measurements and the thermodynamic analysis, we infer that the interaction of water with the glassy biopolymer occurs on very small length scales, i.e., water is closely associated with the carbohydrate residues. It influences the average hole size by a combination of two effects. First, water tends to fill the smallest voids in the glassy matrix. Second, the absorbed water, due to its interference with the intermolecular hydrogen bonding of the carbohydrates, increases the number of degrees of freedom of the carbohydrate chains leading to a "cold" relaxation of the chains and coalescence of the smallest voids under the driving force associated with the reduction of free surface area (i.e. the surface tension).

Our findings explain a number of important related properties of carbohydrates. In the dry state, carbohydrate polymers have a glass transition temperature, which is much higher than that of virtually all synthetic polymers of similar molecular weight.[25] One qualitative picture explaining both the high glass transition temperature of amorphous carbohydrates and the plasticizing effect of water is thus clear: in the dry state, the formation of intermolecular hydrogen bonds between the carbohydrate molecules leads to formation of larger molecular entities, whereas water disrupts the formation of hydrogen bonds between the carbohydrate chains. This picture is to some extent confirmed by recent computer simulations.[21,26,27] Because of the difficulties in probing hydrogen bonds in carbohydrates,[27−30] only modest progress is seen in the analysis of carbohydrate properties in dense matrices in experiment.[31,32] We experimentally confirm that water in glassy carbohydrates should be described at the smallest structural length scales, in accordance with the important role of hydrogen bonding in the formation of the intermolecular carbohydrate network.

Concluding Remarks

The sorption of water by amorphous carbohydrates and its ensuing plasticization proceeds via a complex mechanism involving both hydrogen bond formation and disruption, and changes in the matrix free volume. An important, so far unknown length scale appears in this process, namely the matrix void size, and its dependence on temperature and water activity. We infer that the initial stages of water sorption proceed via the localized binding of water in small moieties close to the carbohydrate chains influencing the hydrogen bonding of the carbohydrates. We anticipate that our results will give impetus to studies aiming to resolve thus far intractable aspects of the topic, most importantly the quantitative analysis of the dynamics of the hydrogen-bonded carbohydrate network.

Acknowledgment. We are grateful to Maria-Isabelle Alonso, Jean-Pierre Marquet, and Isabelle Bauwens for analytical assistance. We thank Gilles Vuataz for discussions and Alain Fracheboud and his team for help with the preparation of amorphous matrices.

References and Notes

(1) Rey, L.; May, J. C. Freeze-Drying/Lyophilization of Pharmaceutical and Biological Products. *Drugs Pharm. Sci.* **1999**, *96*.

(2) Levine, H. Amorphous Food and Pharmaceutical Systems. *Spec. Publ. R. Soc. Chem.* **2002**, *281*.

(3) Risch, S. J.; Reineccius, G. A. Encapsulation and Controlled Release of Food Ingredients. *ACS Symp. Ser.* **1995**, *590*.

(4) Gibbs, B. F.; Kermasha, S.; Alli, I.; Mulligan, C. N. *Int. J. Food Sci. Nutr.* **1999**, *50*, 213.

(5) Ubbink, J.; Schoonman, A. Flavor Delivery Systems. *Kirk-Othmer Encyclopedia of Chemical Technology*; Wiley: New York, 2003.

(6) Roos, Y. H. *Phase Transitions in Foods*; Academic Press: San Diego, CA, 1995.

(7) Aldous, B. J.; Franks, F.; Greer, A. L. *J. Mater. Sci.* **1997**, *32*, 301.

(8) Tromp, R. H.; Parker, R.; Ring, S. G. *Carbohydr. Res.* **1997**, *303*, 199.
(9) Roberts, C. J.; Debenedetti, P. G. *J. Phys. Chem. B* **1999**, *103*, 7308.
(10) Schoonman, A.; Ubbink, J.; Bisperink, Ch.; Le Meste, M.; Karel, M. *Biotechnol. Prog.* **2002**, *18*, 139.
(11) Gunning, Y. M.; Parker, R.; Ring, S. G. *Carbohydr. Res.* **2000**, *329*, 377.
(12) Brandt, W.; Berko, S.; Walker, W. W. *Phys. Rev.* **1960**, *120*, 1289.
(13) Eldrup, M.; Lightbody, D.; Sherwood, J. N. *Chem. Phys.* **1981**, *63*, 51.
(14) Petrick, R. A. *Prog. Polym. Sci.* **1997**, *22*, 1.
(15) Reiss, H. *Methods of Thermodynamics*; Blaisdell: New York, 1964; Chapter III.
(16) Kirkwood, J. G.; Oppenheim, I. *Chemical Thermodynamics*; McGraw-Hill: New York, 1961; Chapter 11.
(17) Anderson, R. B. *J. Am. Chem. Soc.* **1946**, *68*, 686.
(18) Zimm, B. H.; Lundberg, J. L. *J. Phys. Chem.* **1956**, *60*, 425.
(19) Adamson, A. W. *Physical Chemistry of Surfaces*, 2nd ed.; Interscience: New York, 1967.
(20) Benczédi, D.; Tomka, I.; Escher, F. *Macromolecules* **1998**, *31*, 3055.
(21) Molinero, V.; Çağin, T.; Goddard, W. A. *Chem. Phys. Lett.* **2003**, *377*, 469.
(22) Lourdin, D.; Colonna, P.; Ring, S. G. *Carbohydr. Res.* **2003**, *338*, 2883.
(23) Franks, F. *Water*: *a matrix of life*, 2nd ed.; Royal Society of Chemistry: Cambridge, UK, 2000; Chapter 2.
(24) Benczédi, D.; Tomka, I.; Escher, F. *Macromolecules* **1998**, *31*, 3062.
(25) Van Krevelen, D. W. *Properties of polymers*, 3rd ed.; Elsevier: Amsterdam, The Netherlands, 1990; Chapter 6.
(26) Trommsdorff, U.; Tomka, I. *Macromolecules* **1995**, *28*, 6138.
(27) Kirschner, K. N.; Woods, R. J. *Proc. Natl. Acad. Sci. U.S.A.* **2001**, *98*, 10541.
(28) Jeffrey, G. A.; Saenger, W. *Hydrogen Bonding in Biological Structures*; Springer: Berlin, Germany, 1991; Chapter 13.
(29) Carver, J. P. *Curr. Opin. Struct. Biol.* **1991**, *1*, 716.
(30) Rice, K. G.; Wu, P.; Brand, L.; Lee, Y. C. *Curr. Opin. Struct. Biol.* **1993**, *3*, 669.
(31) Wolkers, W. F.; Oldenhof, H.; Alberda, M.; Hoekstra, F. A. *Biochim. Biophys. Acta* **1998**, *1379*, 83.
(32) Ottenhof, M.-A.; MacNaughtan, W.; Farhat, I. A. *Carbohydr. Res.* **2003**, *338*, 2195.
(33) Tao, S. *J. Chem. Phys.* **1972**, *56*, 5499.